FEBS Letters 581 (2007) 1819–1824

Activation of the unfolded protein response and alternative splicing of ATF6α in HLA-B27 positive lymphocytes

Andrew J. Lemin[1], Khalil Saleki[1], Marcel van Lith, Adam M. Benham*

School of Biological and Biomedical Sciences, University of Durham, South Road, Durham DH1 3LE, England, United Kingdom

Received 2 February 2007; accepted 23 March 2007

Available online 4 April 2007

Edited by Felix Wieland

Abstract Misfolding of major histocompatibility complex (MHC) class I molecules has been implicated in the rheumatic autoimmune disease ankylosing spondylitis (AS), and has been linked to the unfolded protein response (UPR) in rodent AS models. XBP1 and ATF6α are two important transcription factors that initiate and co-ordinate the UPR. Here we show that misoxidised MHC class I heavy chains activate XBP1 processing in a similar manner to tunicamycin, with tunicamycin and dithiothreitol (DTT) inducing differential XBP1 processing. Unexpectedly, ATF6α mRNA is alternatively spliced during reducing stress in lymphocytes. This shorter ATF6α message lacks exon 7 and may have a regulatory role in the UPR.

Keywords: Endoplasmic reticulum; Unfolded protein response; MHC; Transcription factor; Protein folding

1. Introduction

Controlled protein secretion by specialized cells like the B cell requires the co-ordinated synthesis of endoplasmic reticulum (ER) membranes, chaperones and folding factors. Terminally misfolded proteins in the ER must be removed to prevent chronic intracellular indigestion and the onset of apoptosis, and this is monitored by the unfolded protein response (UPR) [1]. The eukaryotic UPR consists of a number of specialized signaling molecules, including IRE1 [2], ATF6α [3,4] and the transcription factor XBP1 [5]. XBP1 binds upstream of a UPR target gene to initiate transcription, but only after it has been activated by unconventional mRNA processing. Activation of XBP1 mRNA is achieved by IRE1, which dimerises, autophosphorylates, and becomes active as a site-specific endo-RNase when unfolded proteins accumulate in the ER [6,7]. IRE1 is likely to bind unfolded proteins directly and is kept in the inactive (monomeric) form by BiP.

Whereas XBP1 is a cytosolic/nuclear transcription factor that is activated by IRE1, ATF6α can sense and initiate UPR gene transcription directly. ATF6α is a member of the ATF/CREB family of bZIP proteins [8] and the protein is cleaved in the Golgi by regulated intra-membrane proteolysis [9]. Stress-induced cleavage of the ATF6α precursor occurs after dissociation from BiP [10], releasing a cytosolic fragment. This liberated transcription factor can bind to consensus ERSE sequences (with NF-Y) upstream of target genes [11]. ATF6α can initiate XBP1 expression [5], and can dimerise with other transcription factors such as SRF [3], SREBP2 [12] and CREB-H [13].

Recently, ER stress has been proposed to be involved in ankylosing spondylitis (AS) [14], an arthritic condition in which most sufferers express the HLA-B27 allele of the major histocompatibility complex (MHC) class I family [15]. Although HLA-B27 homodimers at the cell surface may have altered signaling properties [16,17], HLA-B27 can also misfold in the ER and could trigger the UPR [18–20]. However, it is not clear how UPR initiation might result in disease, or how findings from animal models relate to the clinic. To investigate whether MHC class I molecules cause an UPR in humans, we have examined HeLa cells expressing misfolded HLA-B2705. We find that over expression of MHC class I heavy chains is sufficient to induce the UPR and that HLA-B27 positive lymphocytes are pre-sensitised to XBP1 splicing compared to the monocyte cell line THP1. Dithiothreitol, but not tunicamycin, induces a long lasting UPR that culminates in the alternative splicing of ATF6α in lymphocytes. Our results show that UPR induction by faulty glycosylation and UPR induction by disulfide bond reduction can be discriminated at the level of both XBP1 processing and ATF6α transcription.

2. Materials and methods

2.1. Cell lines and constructs

The human lymphoblastoid cell lines JESTHOM, HOM-2 (both HLA-B2705) and WEWAK1(HLA-B2704) were obtained from the ECACC. The human acute monocytic leukaemia cell line THP1 was a gift from J. Robinson, Newcastle University, UK. These cell lines were cultured in RPMI 1640 (Invitrogen). The human cervical carcinoma cell line HeLa was maintained in minimum essential medium. All cell lines were supplemented with 8% FCS, 100 units ml^{-1} penicillin, 100 μg ml^{-1} streptomycin and 2 mM glutamax. The cDNA encoding wild-type HLA-B2705 (confirmed by DNA sequencing) and the HC10 monoclonal antibody recognising free MHC class I heavy chains were gifts from J. Neefjes, Netherlands Cancer Institute.

*Corresponding author. Fax: +44 191 334 1201.
E-mail address: Adam.benham@durham.ac.uk (A.M. Benham).

[1]Authors K.S. and A.J.L. contributed equally to this manuscript.

Abbreviations: AS, ankylosing spondylitis; DTT, dithiothreitol; ER, endoplasmic reticulum; ERSE ER, stress response element; GAMPO, goat anti-mouse peroxidase; HLA, human leukocyte antigen; LPS, lipopolysaccharide; MHC, major histocompatibility complex; NEM, *N*-ethylmaleimide; PMA, phorbol myristate acetate; PVDF, polyvinylidene fluoride; RT-PCR, reverse transcriptase polymerase chain reaction; UPR, unfolded protein response

0014-5793/$32.00
doi:10.1016/j.febslet.2007.03.069

2.2. Cell treatments

Suspension cells were grown to a density of ~2–10 × 10^5 cells ml^{-1} and resuspended with fresh medium containing 10 mM DTT or 10 μg ml^{-1} tunicamycin to induce ER stress for given times. THP1 cells were treated with 20 μg ml^{-1} LPS for 4 days to induce partial differentiation to adherent macrophages. Adherent HeLa cells were supplemented with 10 mM DTT or 10 μg ml^{-1} tunicamycin for 6 h.

2.3. Cell transfections and lysis

HeLa cells in 6 cm dishes were transfected with 1 μg DNA in the presence of 5 μl lipofectamine 2000 for 6 h in optiMEM (Invitrogen). Cells were then provided with complete medium and analysed 24 h post-transfection. Cells were lysed at 4 °C in 300 μl MNT lysis buffer (20 mM MES, 100 mM NaCl, 30 mM Tris, pH 7.4, supplemented with 20 mM *N*-ethylmaleimide (NEM), 1% Triton X-100 and 10 μg/ml each of chymostatin, leupeptin, antipain, and pepstatin A). Post-nuclear supernatants were taken up in sample buffer in the presence (reducing) or absence (non-reducing) of 50 mM DTT and then subjected to 8% SDS–PAGE.

2.4. Western blotting

Gels were wet transferred to polyvinylidene fluoride (PVDF) membranes (Millipore) for 2 h at 150 mA and the membranes were blocked in 8% milk in PBS–Tween for 1 h. Membranes were incubated with HC10 (1:200 tissue culture supernatant) for 1 h before being washed five times with PBS–Tween. Membranes were then incubated with goat anti-mouse peroxidase (GAMPO) secondary antibodies (DAKO) at 1:3000 for 1 h, and subsequently washed five times with PBS–Tween. Proteins were then visualised with 200 μl enhanced chemiluminescence fluid (Amersham) per membrane and exposed to film (Kodak).

2.5. Primers

The primers used for reverse transcriptase polymerase chain reaction (RT-PCR) were as follows:
ATF6α: TGATGCCTTGGGAGTCAGAC and GTGTCAGAGAACCAGAGGCT.
XBP1: GAAACTGAAAAACAGAGTAGCAGC and GCTTCCAGCTTGGCTGATG.
Actin: CCACACCTTCTACAATGAGC and ACTCCTGCTTGCTGATCCAC.

2.6. RT-PCR, XBP1 analysis and sequencing of ATF6α

Cells were lysed in TRI reagent (Sigma) and the concentration of extracted, precipitated RNAwas determined by spectrophotometry. Fifty nanograms total cell RNA was subjected to RT-PCR using the Access-Quick RT-PCR kit (Promega). XBP1 cDNA was subjected to *Pst*I digestion for 2 h at 37 °C and DNA extracted using a PCR purification kit (Qiagen). All cDNA was either analysed by 1% or 2% agarose gel at 100 mV for ~50 min before visualising by UV light. ATF6α RT-PCR products were purified using the QIAquick gel extraction kit (Qiagen) and sequenced by the departmental sequencing centre. White-on-black images were inverted in Adobe Photoshop.

3. Results

3.1. Differential activation of XBP1 by DTT and tunicamycin

Prior to analyzing the relationship between HLA-B27 and the UPR, we optimized UPR induction by stimulating the human monocyte cell line THP1 with either tunicamycin or DTT for 0, 3, 6 and 24 h. We took advantage of the fact that activation (splicing) of XBP1 results in the removal of a unique *Pst*I site from the mRNA transcript [7]. Thus the UPR is activated if a higher molecular weight (undigested) band is observed on agarose gels after incubation of the cDNA with *Pst*I. The fragments expected from this digestion are explained in Fig. 1A. In the absence of DTT or tunicamycin, XBP1 was not spliced, resulting in a *Pst*I sensitive product that was digested into two fragments of 289 and 255 nucleotides (Fig. 1B, lanes 1 and 5). Both DTT and tunicamycin induced XBP1 mRNA processing in THP1 cells (Fig. 1B, lanes 2 and 6). However, tunicamycin stimulation resulted in a resistant species that ran as a doublet (S) and persisted as a singlet after 24 h (Fig. 1B, lane 4). In contrast, DTT stimulation resulted in a single resistant species that ran at the same height as the lower band in the tunicamycin stimulated doublet (Fig. 1B, lanes 6–8). THP1 cells partially recovered from tunicamycin stimulation after 24 h, whereas in DTT stimulated cells, XBP1 remained processed after this time (Fig. 1, compare lanes 4 and 8), despite the fact that DTT is a labile reductant that likely becomes oxidized in the culture medium. Lower concentrations of DTT also triggered the appearance of a single XBP1 band (not shown). These results suggest that XBP1 splicing can follow more than one pathway, and that DTT and tunicamycin can activate subtly different processing or RNA ligation events upstream of XBP1.

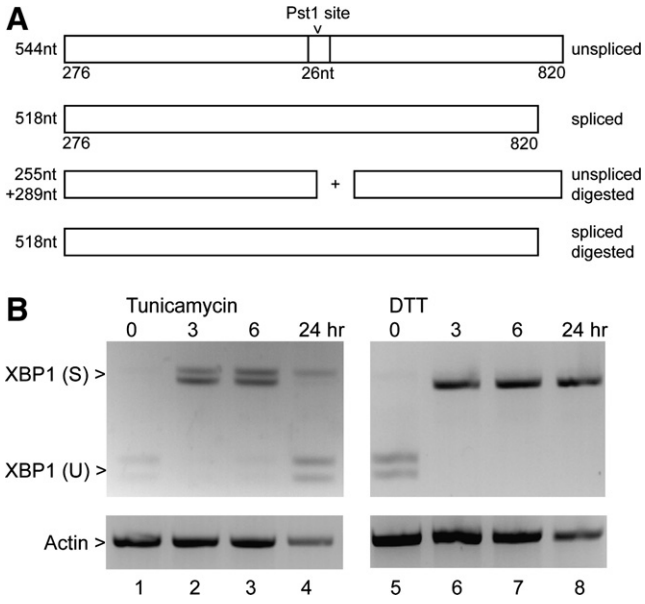

Fig. 1. Induction of XBP1 processing by DTT and tunicamycin. (A) Diagram illustrating the two expected mRNA/cDNA products of XBP1, and their digestions by *Pst*I. The unique *Pst*I site is removed when XBP1 is processed. (B) THP1 cells treated with (lanes 2–4) and without (lane 1) 10 μg ml^{-1} tunicamycin or with (lanes 6–8) and without (lane 5) 10 mM DTT were lysed in TRI reagent, and the lysates subjected to RT-PCR to detect XBP1. Resultant cDNA was digested with *Pst*I and analysed by 2% agarose gel to visualize the activated spliced (S) and unspliced (U) products. Actin was used as a control (lower panel).

3.2. Misoxidised MHC class I heavy chains induce XBP1 processing in HeLa cells

UPR activation has been linked to misfolding of HLA-B2705 heavy chains in a rat model of AS [14]. Thus we investigated whether misoxidised HLA-B2705 could activate the UPR in HeLa cells. MHC class I heavy chains require both an accessory light chain protein, β2m, and a peptide to fold properly in the ER [21] and we have previously shown that over expressed heavy chains misoxidise and form abundant disulfide linked complexes in HeLa cells [22]. HeLa cells transfected (or mock transfected) with HLA-B2705 were simultaneously lysed in the presence of the alkylating agent NEM to preserve disulfide bonds or were taken up in TRI reagent for

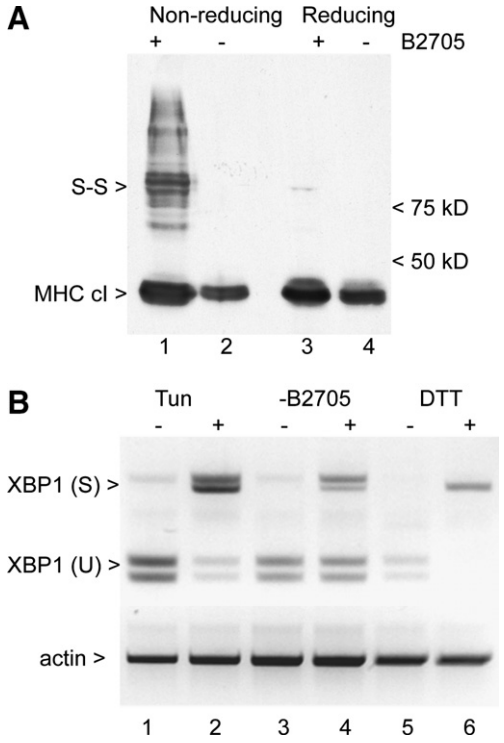

Fig. 2. Misoxidised MHC class I heavy chains induce a tunicamycin-like pathway of XBP1 processing. (A) HeLa cells transfected (lanes 1 and 3) or mock transfected (lanes 2 and 4) with HLAB2705 were lysed 24 h post-transfection and the supernatants subjected to non-reducing (lanes 1 and 2) and reducing (lanes 3 and 4) 8% SDS–PAGE prior to immunoblotting with HC10 to detect MHC class I protein heavy chains. (B) HeLa cells treated for 6 h with (lane 1) or without (lane 2) tunicamycin, with (lane 6) or without (lane 5) DTT, or 24 h post-transfection with (lane 4) or without (lane 3) HLAB2705 were lysed with TRI reagent and the mRNA subjected to RT-PCR and *Pst*I digest. 2% agarose gel electrophoresis was used to detect spliced (S) and unspliced (U) XBP1 products. Actin was used as a positive control (lower panel).

subsequent RT-PCR analysis. Upon non-reducing SDS–PAGE, the HLA-B2705 transfected cells showed a ladder of MHC class I complexes (Fig. 2A, lane 1), which could be resolved into a single species by adding DTT to reduce the samples (Fig. 2A, lane 3), confirming that the MHC heavy chains were misoxidised.

In THP1 cells, induction of the UPR by DTT resulted in a single, activated XBP1 *Pst*I resistant product, whereas activation of the UPR by tunicamycin resulted in a doublet (Fig. 1B, compare lanes 2 and 6). In HeLa cells, treatment with DTT or tunicamycin also induced the UPR and resulted in the generation of the same *Pst*I resistant (active) forms of XBP1, showing that differences in the processing of XBP1 were reproducible between different cell lines (Fig. 2B, lanes 1, 2, 5 and 6). Note that the tunicamycin (S) doublet cannot be explained by incomplete digestion or polymorphism at the *Pst*I site because there is no prominent (S) band in the undigested samples (Fig. 2B, lane 1). In contrast to mock transfectants (Fig. 2B, lane 3), HeLa cells expressing misoxidised HLA-B2705 generated XBP1 mRNA in the *Pst*I resistant (activated) form. This *Pst*I resistant material appeared as a doublet (Fig. 2B, lane 4). Thus misoxidation of MHC class I heavy chains is sufficient to induce the UPR via a tunicamycin-like pathway of XBP1 splicing.

3.3. XBP1 processing in HLA-B27 positive lymphocytes

We next investigated the status of XBP1 in HLA-B27 typed lymphoblastoid cell lines, one of which was HLA-B2704 positive (WEWAK1), and two of which were HLA-B2705 positive (JESTHOM and HOM-2) and known to come from AS positive donors. We examined the sensitivity of these lymphocytes to UPR induction with both tunicamycin and DTT (Fig. 3). As a negative control, we used THP1 cells treated with of without LPS only for 4 days. Both LPS and PMA stimulation are required to induce a UPR in monocytes [23]. LPS stimulated the differentiation of THP1 to the adherent macrophage-like state, but did not result in nonspecific activation of XBP1 (Fig. 3A, compare lanes 10 and 11). Compared with THP1 cells, WEWAK1, HOM-2 and JESTHOM all showed higher levels of XBP1 splicing in the absence of any applied stimuli (Fig. 3A, compare lanes 1, 4 and 7 with lane 10). DTT fully activated XBP1 splicing in these cell lines (Fig. 3A, lanes 2, 5 and 8), whereas tunicamycin caused only a small increase compared to the untreated control (Fig. 3A, lanes 3, 6 and 9). The DTT induced splice form always ran at the level of the lower band of the tunicamycin-induced doublet, consistent with HeLa cells (Figs. 1 and 2) and THP cells (see Fig. 4).

To investigate these size differences further, the individual *Pst*I resistant PCR products obtained after treating HeLa cells with DTT, or WEWAK1 cells with DTT or tunicamycin were excised from 2% agarose gels, separated out (Fig. 3B) and re-analysed for sequencing. The insertion resulting in the top PCR product (Fig. 3B, lane 3) proved refractory to reproducible sequencing analysis, using a number of different primer sets (data not shown). However, the lower tunicamycin-induced band (Fig. 3B, lane 4) was identical in sequence to the DTT-induced PCR product (Fig. 3B, lanes 1 and 2), with an excised 26 bp sequence bridging the *Pst*I site (Fig. 3C). This result was confirmed in both HeLa and WEWAK1 cells, and is consistent with the literature [7]. We conclude from our experiments that the lymphocyte cell lines examined have a higher degree of baseline UPR activation than THP1 cells. XBP1 activation in these cells results in a novel *Pst*I resistant splice form, comparable to that induced by tunicamycin, rather than DTT. Whether this effect is caused by chronic, low-level misfolding of HLA-B27, or is due to other factors will require further investigations using fresh patient cells.

3.4. Alternative splicing of ATF6α is induced by DTT

The differences between XBP1 processing induced by tunicamycin and DTT led us to investigate whether other branches of the UPR were differently affected by ER stress in lymphocytes [24]. Unlike XBP1, activation of ATF6α occurs by liberating an active transcription factor by proteolysis at the protein level. However, whilst examining RNA levels of ATF6α during UPR, we found that an additional PCR product could be detected in lymphoblastoid cells that had been treated with DTT, but not in cells that had been treated with tunicamycin (Fig. 4). This product was most prominent in WEWAK1 cells (Fig. 4A, lane 2) but could also be detected in the AS cell line JESTHOM (Fig. 4A, lane 8), and very weakly in HOM-2 (Fig. 4A, lane 5). This product was not detectable in negative-control (LPS stimulated) THP1 cells (Fig. 4A, lane 11) or in DTT and tunicamycin-stimulated THP1 cells (Fig. 4B), although XBP1 splicing could be induced by DTT and tunicamycin in the monocytic THP1 cell line (Fig. 4C).

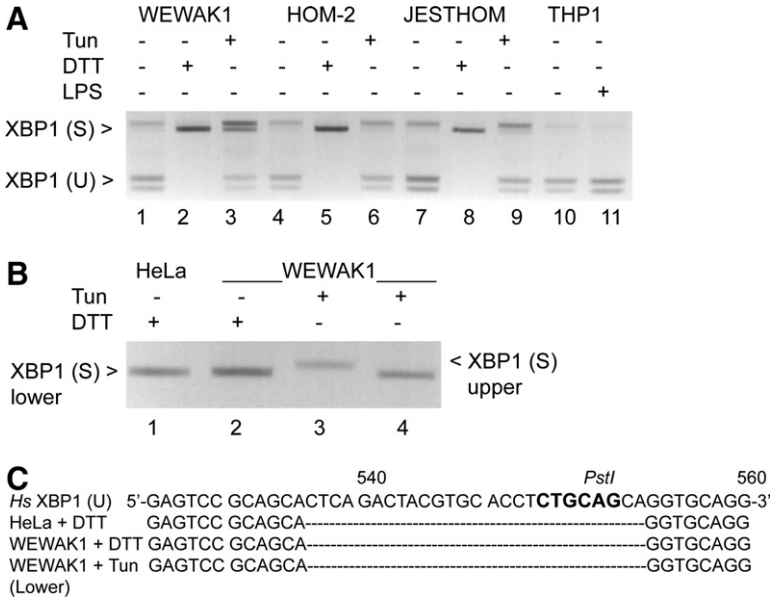

Fig. 3. Activation of the UPR in HLA-B27 positive lymphoblastoid cell lines. (A) WEWAK1 (lanes 1–3), HOM-2 (lanes 4–6), JESTHOM (lanes 7–9) and THP1 cells (lanes 10 and 11) were mock treated (lanes 1, 4, 7 and 10), treated with 10 mM DTT (lanes 2, 5 and 8) or 10 μg ml^{-1} tunicamycin (lanes 3, 6 and 9) for 6 h. THP1 cells treated with 20 μg ml^{-1} LPS for 4 days were used as a negative control (lane 11). Cells were lysed in TRI reagent and mRNAs were subjected to RT-PCR and *Pst*I digest prior to 2% agarose gel electrophoresis to detect spliced (S) and unspliced (U) XBP1 products. (B) The discrete *Pst*I resistant XBP1 PCR products from HeLa cells treated with 10 mM DTT (lane 1), and those from WEWAK1 cells treated with 10 mM DTT (lane 2) or 10 μg ml^{-1} tunicamycin (lanes 3 and 4) were re-analysed by 2% agarose gel electrophoresis. (C) The XBP1 products from (B) were sequenced, with lanes 1, 2 and 4 confirmed as XBP1 with an excised 26 bp sequence in the region of the *Pst*I site.

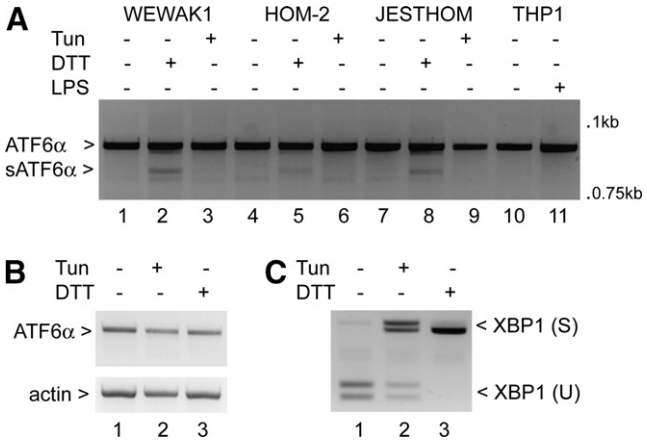

Fig. 4. Alternative splicing of ATF6α is induced by DTT. (A) WEWAK1 (lanes 1–3), HOM-2 (lanes 4–6), JESTHOM (lanes 7–9) and THP1 cells (lanes 10 and 11) were mock treated (lanes 1, 4, 7 and 10), or treated with 10 mM DTT (lanes 2, 5 and 8) or 10 μg ml^{-1} tunicamycin (lanes 3, 6 and 9) for 6 h. THP1 cells treated with 20 μg ml^{-1} LPS for 4 days were used as a negative control (lane 11). mRNAs were subjected to RT-PCR and 2% agarose gel electrophoresis to detect ATF6α products. (B) THP1 cells were mock treated (lane 1), treated with 10 μg ml^{-1} tunicamycin (lane 2) or 10 mM DTT (lane 3) for 6 h, followed by lysis in TRI reagent and RT-PCR to detect ATF6α (upper panel) and actin (lower panel) using 2% agarose gel electrophoresis. (C) As for (B) but using RT-PCR to detect XBP1.

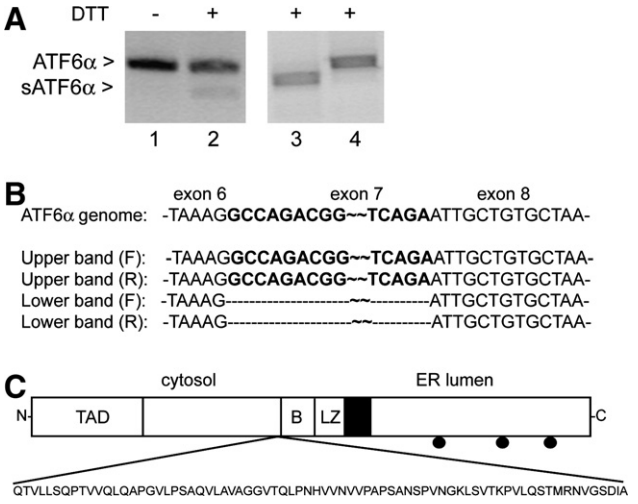

Fig. 5. The short form of ATF6α lacks exon 7. (A) The mRNA from WEWAK1 cells stimulated for 6 h in the presence (lanes 2, 3 and 4) or absence (lane 1) of 10 mM DTT was subjected to RT-PCR to detect and isolate the short and conventional forms of ATF6α prior to analysis by 2% agarose gel electrophoresis. (B) Sequence of the upper band and lower band from (A) with both forward (F) and reverse (R) primers. Bold type represents a section of the nucleotide sequence present in the upper product and absent in the lower product, corresponding to the known sequence of exon 7. The sizes of the sequenced products are consistent with agarose gel analysis, where the 1 kb marker runs just above the major ATF6α product and the 0.75 kb marker runs just below the short form. (C) Schematic diagram of the ATF6α protein showing the amino acid sequence that is missing when exon 7 is spliced out. TAD = transcription activation domain, B = DNA binding domain, LZ = leucine zipper, dark shading = ER transmembrane sequence, circles = glycosylation sites.

To identify the DTT-induced ATF6α product, which we termed (short) sATF6α, the upper and lower bands were cut out from the agarose gel (Fig. 5A, lane 2), purified, reamplified by PCR (Fig. 5A, lanes 3 and 4) and sequenced. DNA sequencing revealed that sATF6α lacked exon 7, but otherwise was identical in sequence to the upper band, which matched the ATF6α sequence found in the database (Fig. 5B). This alternative splicing event appeared specific to ATF6α, since

we could not detect a similar DTT-induced product when primers for the ATF6α homolog ATF6β were used for RT-PCR analysis (not shown). We conclude that induction of the UPR by DTT (but not by tunicamycin) results in alternative splicing of ATF6α in lymphocytes. This creates a shorter protein that lacks 75 amino acids at the boundary of the DNA binding domain (Fig. 5C) and may be a novel participant in the regulation of the UPR.

4. Discussion

We have shown that over-expression of MHC class I heavy chains stimulates the UPR (Fig. 2). XBP1 shows some pre-activation in three HLA-B27 expressing lymphoblastoid cell lines, giving an induction pattern similar to that induced by a glycosylation inhibitor (tunicamycin) rather than that induced by a reductant of disulfide bonds (DTT) (Fig. 3). Our results suggest that tunicamycin stimulation is a better mimic of UPR induction by MHC class I misoxidation (Figs. 1 and 3). It will be important to determine the molecular signature of the *Pst*I resistant XBP1 species that is induced upon heavy chain misoxidation or tunicamycin treatment. Whether it is IRE1 RNase activity, or the two alternative mammalian ligase activities, that give rise to these different XBP1 products should also be addressed by future experiments. Although HLA-B2705 and HLA-B2704 are linked to AS, our results do not point to a simple relationship between HLA-B27 and UPR induction. It is more likely that there is a complex role for the UPR in AS *in vivo*, where cytokines and the inflammatory response are involved. Furthermore, professional antigen presenting cells (e.g. dendritic cells) or endothelial cells at the rheumatic joint may behave differently to the immortalized lymphocytes examined here.

We have shown for the first time that ATF6α is subject to alternative splicing during reducing ER stress, but not during tunicamycin-induced ER stress or in THP1 cells (Fig. 4). We have sequenced sATF6α and shown that it lacks exon 7 (Fig. 5). The cell specificity, biological activity and precise function of sATF6α remain to be determined. However, since exon 7 lies at the start of the bZIP DNA binding domain, we predict that the shortened form of the ATF6 protein may have altered dimerisation and/or transcriptional activation properties. Although sATF6α is generated upon DTT treatment, cells continue to express fulllength ATF6α. Thus redox stress does not cause a complete switch from the full-length form to the shorter form. Rather, sATF6α may compete with ATF6α to reduce promoter occupancy, or could sequester ATF6α (as dimers) away from promoter elements. There is evidence that both these mechanisms can regulate the mammalian UPR in other circumstances: ATF6β has low transcriptional activity [25], and represses ATF6α in competition experiments when target gene expression is driven from an ERSE [26]. Unspliced XBP1 can also regulate the activity of spliced XBP1 by targeting the XBP1 complex to the proteasome for degradation [27]. It is also possible that induction of sATF6α is involved in regulating entry into programmed cell death.

It is worth noting that endogenous alternatively spliced ATF6α will not be detected by anti-tag antibodies commonly used to identify ATF6α proteins in transfection experiments. Thus a short form of ATF6α could explain some discrepancies between UPR activation and mRNA levels of target transcripts [28], particularly if DTT is used as a UPR inducer. Recent work has shown that at the protein level, UPR components react differently to assorted UPR activators [24]. Our experiments have revealed a hitherto unknown splicing event that demonstrates that ATF6α is processed at both the protein and mRNA level during an ER stress response. Given that inflammation and the UPR can act synergistically [13], the inability to reset the UPR after chronic stimulation may be an important component of diseases such as AS, rather than simply the induction of the UPR itself.

Acknowledgements: We thank Martin Schröder for critical comments on the manuscript, the arthritis research campaign and the BBSRC for funding, and John Robinson and Jacques Neefjes for cell lines and antibodies.

References

[1] Schroder, M. and Kaufman, R. (2005) The mammalian unfolded protein response. Annu. Rev. Biochem. 74, 739–789.
[2] Wang, X.Z., Harding, H.P., Zhang, Y., Jolicoeur, E.M., Kuroda, X. and Ron, D. (1998) Cloning of mammalian Ire1 reveals diversity in the ER stress responses. EMBO J. 17, 5708–5717.
[3] Zhu, C., Johansen, F. and Prywes, R. (1997) Interaction of ATF6 and serum response factor. Mol. Cell. Biol. 17, 4957–4966.
[4] Haze, K., Yoshida, H., Yanagi, H., Yura, T. and Mori, K. (1999) Mammalian transcription factor ATF6 is synthesized as a transmembrane protein and activated by proteolysis in response to endoplasmic reticulum stress. Mol. Biol. Cell 10, 3787–3799.
[5] Yoshida, H., Matsui, T., Yamamoto, A., Okada, T. and Mori, K. (2001) XBP1 mRNA is induced by ATF6 and spliced by IRE1 in response to ER stress to produce a highly active transcription factor. Cell 107, 881–891.
[6] Tirasophon, W., Lee, K., Callaghan, B., Welihinda, A. and Kaufman, R.J. (2000) The endoribonuclease activity of mammalian IRE1 autoregulates its mRNA and is required for the unfolded protein response. Genes Dev. 14, 2725–2736.
[7] Calfon, M., Zeng, H., Urano, F., Till, J.H., Hubbard, S.R., Harding, H.P., Clark, S.G. and Ron, D. (2002) IRE1 couples endoplasmic reticulum load to secretory capacity by processing the XBP-1 mRNA. Nature 415, 92–96.
[8] Hai, T. and Hartman, M.G. (2001) The molecular biology and nomenclature of the activating transcription factor/cAMP responsive element binding family of transcription factors: activating transcription factor proteins and homeostasis. Gene 273, 1–11.
[9] Ye, J., Rawson, R.B., Komuro, R., Chen, X., Dave, U.P., Prywes, R., Brown, M.S. and Goldstein, J.L. (2000) ER stress induces cleavage of membrane-bound ATF6 by the same proteases that process SREBPs. Mol. Cell 6, 1355–1364.
[10] Shen, J., Chen, X., Hendershot, L. and Prywes, R. (2002) ER stress regulation of ATF6 localization by dissociation of BiP/GRP78 binding and unmasking of Golgi localization signals. Dev. Cell 3, 99–111.
[11] Yamamoto, K., Yoshida, H., Kokame, K., Kaufman, R.J. and Mori, K. (2004) Differential contributions of ATF6 and XBP1 to the activation of endoplasmic reticulum stress-responsive *cis*-acting elements ERSE, UPRE and ERSE-II. J. Biochem. (Tokyo) 136, 343–350.
[12] Zeng, L., Lu, M., Mori, K., Luo, S., Lee, A.S., Zhu, Y. and Shyy, J.Y. (2004) ATF6 modulates SREBP2-mediated lipogenesis. EMBO J. 23, 950–958.
[13] Zhang, K., Shen, X., Wu, J., Sakaki, K., Saunders, T., Rutkowski, D.T., Back, S.H. and Kaufman, R.J. (2006) Endoplasmic reticulum stress activates cleavage of CREBH to induce a systemic inflammatory response. Cell 124, 587–599.
[14] Turner, M.J. et al. (2005) HLA-B27 misfolding in transgenic rats is associated with activation of the unfolded protein response. J. Immunol. 175, 2438–2448.
[15] Ramos, M. and de Castro, J.A.L. (2002) HLA-B27 and the pathogenesis of spondyloarthritis. Tissue Antigens 60, 191–205.

[16] Allen, R.L., Raine, T., Haude, A., Trowsdale, J. and Wilson, M.J. (2001) Cutting edge: leukocyte receptor complex-encoded immunomodulatory receptors show differing specificity for alternative HLA-B27 structures. J. Immunol. 167, 5543–5547.
[17] Kollnberger, S. et al. (2004) HLA-B27 heavy chain homodimers are expressed in HLA-B27 transgenic rodent models of spondylarthritis and are ligands for paired Ig-like receptors. J. Immunol. 173, 1699–1710.
[18] Dangoria, N.S., DeLay, M.L., Kingsbury, D.J., Mear, J.P., Uchanska-Ziegler, B., Ziegler, A. and Colbert, R.A. (2002) HLA-B27 misfolding is associated with aberrant intermolecular disulfide bond formation (dimerization) in the endoplasmic reticulum. J. Biol. Chem. 277, 23459–23468.
[19] Bird, L.A., Peh, C.A., Kollnberger, S., Elliott, T., McMichael, A.J. and Bowness, P. (2003) Lymphoblastoid cells express HLA-B27 homodimers both intracellularly and at the cell surface following endosomal recycling. Eur. J. Immunol. 33, 748–759.
[20] Antoniou, A.N., Ford, S., Taurog, J.D., Butcher, G.W. and Powis, S.J. (2004) Formation of HLA-B27 homodimers and their relationship to assembly kinetics. J. Biol. Chem. 279, 8895–8902.
[21] Elliot, T. and Williams, A. (2005) The optimization of peptide cargo bound to MHC class I molecules by the peptide-loading complex. Immunol. Rev. 207, 89–99.
[22] Saleki, K., Hartigan, N., van Lith, M., Bulleid, N. and Benham, A.M. (2006) Differential oxidation of HLA-B2704 and HLA-B2705 in lymphoblastoid and transfected adherent cell lines. Antioxid. Redox Signal. 8, 292–299.
[23] Goodall, J.C., Ellis, L., Yeo, G.S.H. and Gaston, J.S.H. (2007) Does HLA-B27 influence the monocyte inflammatory response to lipopolysaccharide? Rheumatology 46, 232–237.
[24] DuRose, J.B., Tam, A.B. and Niwa, M. (2006) Intrinsic capacities of molecular sensors of the unfolded protein response to sense alternate forms of endoplasmic reticulum stress. Mol. Biol. Cell 17, 3095–3107.
[25] Lee, A.-H., Iwakoshi, N.N. and Glimcher, L.H. (2003) XBP-1 regulates a subset of endoplasmic reticulum resident chaperone genes in the unfolded protein response. Mol. Cell. Biol. 23, 7448–7459.
[26] Thuerauf, D.J., Morrison, L. and Glembotski, C.C. (2004) Opposing roles for ATF6a and ATF6b in endoplasmic reticulum stress response gene induction. J. Biol. Chem. 279, 21078–21084.
[27] Yoshida, H., Oku, M., Suzuki, M. and Mori, K. (2006) pXBP1(U) encoded in XBP1 pre-mRNA negatively regulates unfolded protein response activator pXBP1(S) in mammalian ER stress response. J. Cell Biol. 172, 565–575.
[28] Shang, J. and Lehrman, M.A. (2004) Discordance of UPR signaling by ATF6 and Ire1p-XBP1 with levels of target transcripts. Biochem. Biophys. Res. Commun. 317, 390–396.